Third Workshop on Benchmark Problems for Airframe Noise Computations (BANC-III)

14–15 June 2014, Atlanta, Georgia, USA

Workshop Category 1: Trailing-Edge Noise

M. Herr*, C. Bahr[§] and M. Kamruzzaman[‡]

*German Aerospace Center, DLR, michaela.herr@dlr.de
§NASA Langley Research Center, Hampton, VA 23681
‡ ENERCON GmbH, D-26605 Aurich, Germany

1 Overview

The objective of this workshop problem is to assess the present computational capability in the area of physics-based prediction of broadband turbulent boundary-layer trailing-edge (TBL-TE) noise and to advance the state-of-the-art via a combined effort.

To collectively push the state-of-the-art well beyond the current level we kindly invite applications from users of the various concurrent TBL-TE noise prediction approaches, covering the full bandwidth of existing semi-empirical, theoretical and hybrid methods, e.g. approaches based on acoustic analogy or CAA (computational aeroacoustics) in combination with unsteady Reynolds-averaged Navier-Stokes (URANS), large eddy simulation (LES), detached eddy simulation (DES) or RANS with stochastic turbulence models.

1.1 Motivation

TBL-TE noise represents an important issue for the aeroacoustic research community as the related mechanism expresses in a wide range of technical situations like the noise generation at aircraft high-lift systems, at turbo machinery components, cooling fans or wind turbine blades. Validated methods to simulate TBL-TE noise are fundamental for low-noise profile shape optimization and to assist the further development of noise reduction methodologies. Up to now, no single experiment has collected all the data required to fully validate a prediction, and considerable discrepancies exist when considering multiple experiments of similar airfoils [1], [6]. Even if quiet anechoic test facilities are used the generally low signal-to-noise ratios require application of focusing measurement techniques or specified correlation methods. As a consequence, extraction of TBL-TE noise from measured data is based on extensive system-inherent, facility-dependent corrections which themselves have never been perfectly validated so far.

Therefore, it will be instructive to both experimentalists and numericists in academia and industry to elaborate comparisons of the various TBL-TE noise computational methods. To concentrate on the pure broadband TBL-TE noise mechanism and the corresponding numerical issues, i.e. to exclude measurement-related specifics from the numerical results, the problem centers on the computation of flow and noise

generation at sections of 2D airfoils in a nominally uniform stream. Cross-checks with measurement data available for the selected airfoils will help to evaluate the common trends, results, merits and limitations of the different approaches. Moreover, it is hoped that the structure of this problem will provide guidance for future experimental programs attempting to fill the current gaps in airfoil TBL-TE noise validation data.

Due to the existing gaps and uncertainties in airfoil TBL-TE noise validation data **the focus is not on perfectly reproducing the experimental results of a specific data set** (a full numerical simulation including the whole test facility environment could be a future objective of follow-on workshops) **but on code-to-code comparisons** identifying common scaling laws and discrepancies between the various approaches. Nonetheless, the problem statement conditions have been defined with the aim to provide a comparison database that largely covers the full measurement chain from near field source quantities to farfield noise, including the following three distinct sets of experimental data:

1. Steady and unsteady TBL flow properties, including two-point correlations, to verify the numerically predicted or modelled turbulence noise source parameters,
2. TBL-induced unsteady wall pressure spectra close to the TE to assess corresponding prediction models,
3. Farfield TBL-TE noise spectra to finally asses the noise prediction capability.

1.2 Lessons Learnt from BANC-II

The results from BANC-II have been documented in a survey paper presented during last year's AIAA Aeroacoustics conference (AIAA paper 3013-2123):

http://arc.aiaa.org/doi/pdf/10.2514/6.2013-2123.

The (partly incomplete) workshop proceedings can be downloaded here:

https://info.aiaa.org/tac/ASG/FDTC/DG/BECAN_files_/BANCII_proceedings/start_here.html.

1.3 Scope

This document provides

- the definition of simulation parameters and test cases, Sections 2.1 to 2.2,
- reporting instructions, Sections 2.3 to 2.4,
- the documentation of comparison data, Section 3.

BANC-III comparison datasets and templates are identical to the ones used in BANC-II, i.e. can be downloaded at (**file: BANC-II-1.zip**)

https://info.aiaa.org/tac/ASG/FDTC/DG/BECAN_files_/BANCII_category1.

2 Problem Statement

2.1 Parameter Definition and Units

b	m	wetted airfoil span
c_p	-	static pressure coefficient, $c_p = (p-p_\infty)/(0.5\rho_\infty U_\infty^2)$, note the normalization with free stream velocity
c_f	-	wall friction coefficient, $c_f = \tau_W/(0.5\rho_\infty U_\infty^2)$
c_∞	m/s	free stream speed of sound
f	Hz	narrowband frequency
f_c	Hz	1/3-octave band center frequency
k_T	m²/s²	specific kinetic energy of turbulence
l_c	m	chord length
$L_{p(1/3)}$	dB	1/3-octave band trailing-edge noise level (re 20 µPa)
M_∞	-	free stream Mach number
p	Pa	time-averaged surface pressure
p_{rms}	Pa	root-mean-square sound pressure
p_∞	Pa	time-averaged ambient pressure
G_{pp}	dB/Hz	single-sided power spectral density of unsteady surface pressures (levels re 20 µPa); note: measured narrow band spectra of finite band width Δf are normalized to Δf = 1 Hz.
r	m	distance between source position and observer (retarded coordinate system)
$R_{ij}(\xi_i)$	m²/s²	two-point correlations of fluctuation velocities in airfoil-fixed coordinates x_i
T_∞	K	ambient temperature
Re	-	chord-based Reynolds number
U_e	m/s	boundary-layer edge velocity at the TE, derived from the mean velocity profiles as specified in Section 2.3.1, chord-wise velocity at $x_2 = \delta$
U_i	m/s	mean velocity components in airfoil-fixed coordinates x_i
u_i	m/s	fluctuating velocity components in airfoil-fixed coordinates x_i
U_∞	m/s	time-averaged free stream velocity
x_i	m	airfoil-fixed coordinates with origin at the leading edge at midspan (i = 1…3; 1: chordwise, 2: chord-normal, 3: spanwise), cf. Figure 1
α	°	aerodynamical angle of attack, cf. Figure 1
δ	m	boundary layer thickness at the TE, derived from the mean velocity profiles as specified in Section 2.3.1, δ equals x_2, where $U_1(x_2)$ reaches U_e
δ_1	m	boundary layer displacement thickness at the TE:

		$\delta_1 = \int_0^{\delta} 1 - \frac{U_1(x_2)}{U_e}\, dx_2$ (x_2: chord-normal coordinate)
δ_2	m	boundary layer momentum loss thickness at the TE: $\delta_2 = \int_0^{\delta} \frac{U_1(x_2)}{U_e}\left(1 - \frac{U_1(x_2)}{U_e}\right) dx_2$ (x_2: chord-normal coordinate)
ε	m²/s³	isotropic turbulence mean dissipation rate
θ	°	TE observation angle in retarded coordinates, $\theta = 0°$ denotes the downstream chord-aligned direction, $\theta = 90°$ denotes pressure side chord-normal view towards the TE, cf. Figure 1
$\Lambda_{ii,n}(x_2)$	m	integral correlation length scales derived from two-point correlation profiles (index *ii*, *n*: read as length scale of its component of fluctuation velocities u_i for probe separation in *n* direction): $\Lambda_{ii,n}(x_2) = \int_0^{\xi_0} \frac{\langle u_i(\bar{x},t) \cdot u_i(\bar{x}+\bar{\xi},t)\rangle}{\langle u_i^2(\bar{x},t)\rangle} d\bar{\xi} = \int_0^{\xi_0} \tilde{R}_{ii}(\bar{x},\xi_n) d\xi_n$
Λ_f	m	longitudinal integral length scale, cf. Section 2.3
ν_∞	m²/s	ambient kinematic viscosity
ξ_n	m	probe separation coordinate in n-direction (*n* could be x_1, x_2, x_3)
ξ_0	m	location of first zero crossing of $\tilde{R}_{ii}(\bar{x},\xi_n)$, i.e. $\tilde{R}_{ii}(\bar{x},\xi_n = \xi_0) = 0$
ρ_∞	kg/m³	time-averaged ambient density
τ_w	Pa	wall shear stress

2.2 Test Cases

The computation of flow and noise characteristics at sections of 2D airfoils in a nominally uniform stream (U_∞, α) according to Figure 1 is solicited.

Selected test cases are summarized in Table 1.

The definition of these cases has been based on cross comparisons of available data sets including checks for satisfactory quality of the acoustic data. Moreover, the underlying well-documented measurement chains and model hardware have been recently used [10], [14] and are still available for follow-on tests (for BANC-IV, etc.)[1].

The test cases #1 to #4 have been mainly defined based on the availability of measured turbulence length scales (which cannot be easily scaled contrary to noise or surface pressure spectra) and measured transition locations for these conditions [10], [11], [12] (cf. Section 3.1).

[1]Unfortunately, the hardware related to the extensive NASA data sets documented in Refs. [2] and [3] has not been stored why additional tests at different chord lengths would require a larger time frame.

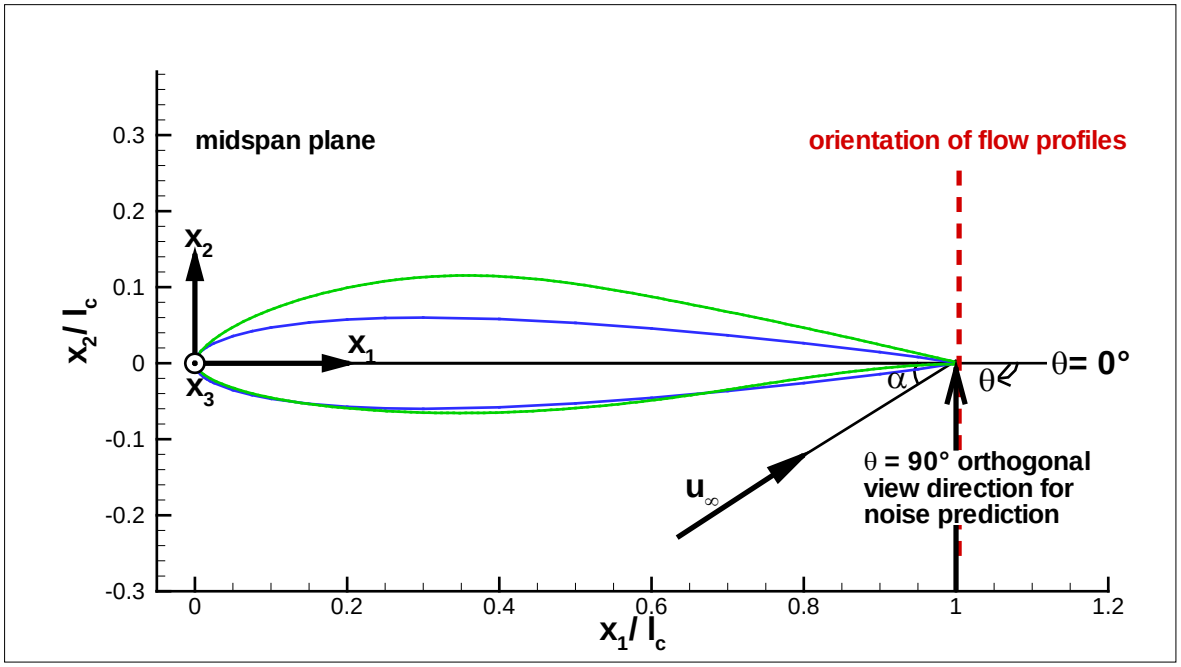

Figure 1: Coordinate system and parameter definition.

Table 1: Simulation matrix (order according to priority; case #1 = single core test case for those submitters who cannot afford to work on the full matrix).

#	Airfoil	l_c, m	Boundary layer fixed transition position, fully turbulent downstream of x_1/l_c (SS: suction side, PS: pressure side)	U_∞, m/s M_∞, - Re, -	T_∞, K ρ_∞, kg/m³ p_∞, Pa	α, °	Availability of comparison data (details will be further specified in Section III of the final paper)
1	**NACA0012**	**0.4**	**SS: 0.065 PS: 0.065**	**56.0 0.1664 1.50 Mio**	**281.5 1.181 95429**	**0**	**$L_{p(1/3)}(f_c)$, $G_{pp}(f)$, flow profiles, $cp(x_1)$**
2	NACA0012	0.4	SS: 0.065 PS: 0.065	54.8 0.1641 1.50 Mio	278.0 1.190 94975	4	$L_{p(1/3)}(f_c)$, $G_{pp}(f)$, flow profiles, $cp(x_1)$
3	NACA0012	0.4	SS: 0.060 PS: 0.070	53.0 0.1597 1.50 Mio	273.8 1.224 96188	6	$L_{p(1/3)}(f_c)$, $G_{pp}(f)$, flow profiles, $cp(x_1)$
4	NACA0012	0.4	SS: 0.065 PS: 0.065	37.7 0.1118 1.00 Mio	283.1 1.171 95156	0	$L_{p(1/3)}(f_c)$, $G_{pp}(f)$, flow profiles
5	DU-96-180	0.3	SS: 0.12 PS: 0.15	60.0 0.1730 1.13 Mio	299.3 1.164 100004	4	$L_{p(1/3)}(f_c)$

Corresponding TBL-TE noise and surface pressure data have been made available by scaling of measured data acquired for conditions close to the problem statement. Case #5 corresponds to the original acoustic measurement conditions [14][2].

If computational resources are a limitation for the method, the highest priority should be given to the angle-of-attack variation for the 0.4-m chord NACA0012 (test cases #1 to #3). **The minimum requirement is to provide simulation results for test case #1.** Although the major objective is to elaborate acoustic predictions, LES/DES-based submissions targeting only the unsteady flow field in the source region will also be accepted.

Airfoil profile coordinates are provided with **zero thickness TE** geometries[3] in the file "\data\BANC-II-1_coordinates.xls". Consider untapered, unswept airfoil sections of a **1-m wetted span**. It is understood that time accurate simulations of the unsteady flow field may be limited to a considerably shorter spanwise domain, e.g. combined with application of periodic boundary conditions. However, to allow a common baseline for comparison between different sets of results, participants are requested to correspondingly scale up their acoustic predictions. The choice of a suitable procedure is left to the participants and should be documented in the final reporting; at minimum a scaling according to $\langle p^2 \rangle \sim b$ (cf. Section 2.3) should be applied.

For the TBL development and hence, TBL-TE noise generation it is important that the measured transition locations x_1/l_c in Table 1 are reproduced in the simulations[4]. The choice of how transition forcing is realized is left to the participants. However, zero inflow turbulence intensity[3] should be considered for all cases. If the simulation approach requires the geometrical resolution of a tripping device participants are encouraged to apply the respectively used experimental measures for transition forcing. For cases #1 to 4 (IAG Stuttgart setup) these were trip strips with a rectangular cross section of 0.36 mm in height and 1.5 mm in width, centered at $x_1/l_c = 0.05$ on both the SS and PS (Figure 2, left). For case #5 (DLR setup) a 0.205-mm Streifeneder zigzag trip strip was used at $x_1/l_c = 0.05$ at the SS and a 0.4-mm Streifeneder zigzag strip at $x_1/l_c = 0.1$ at the PS (here, positions x_1/l_c refer to the tripping leading edge locations, zigzag geometry according to Figure 2, right).

[2]More detailed information about the considered test data and references, the underlying measurement techniques and facilities as well as the applied scaling procedures to scale multiple available data sets according to the problem definition and reporting instructions stated in the following section are provided in Section 3.

[3]Zero TE thickness and zero inflow turbulence intensity are defined herein because the current problem statement concentrates on pure broadband TBL-TE interaction noise; other relevant airfoil noise generation mechanisms like narrow band/ tonal blunt TE vortex shedding noise or turbulent inflow leading edge noise are correspondingly excluded. Tonal laminar vortex-shedding noise as well as flow separation/ deep stall noise are avoided by transition forcing and by moderate angle-of-attack settings.

[4]Effective transition "points" x_1/l_c were measured by means of a stethoscope; these are taken as the position where the boundary layer was fully turbulent; i.e. intermittency regions extend between the leading edge of the tripping device and x_1/l_c. The simulation of intermittency regions is optional.

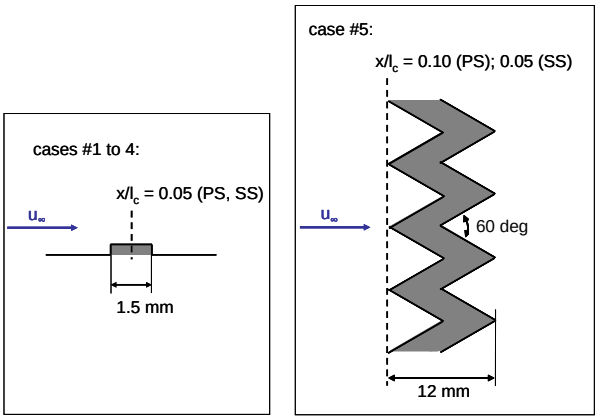

Figure 2: Experimental tripping configurations (for optional use).

2.3. Instructions for Reporting Details

For test cases #1 to #5 participants are requested to calculate the following relevant aerodynamic and acoustic quantities for code to code comparisons (cf. the definitions in Figure 1 and in Section 2.2); experimental comparison data is available for the specifications printed in bold letters:

[1] Farfield <u>one-third-octave band</u> TBL-TE noise spectrum $L_{p(1/3)}(f_c)$ in dB re 20 µPa for b = 1 m and retarded observer positions r, θ of r = 1 m and <u>chord-</u>normal view angle θ = 90° (coordinates according to Figure 1 with origin at the retarded TE source location). If feasible, contributions of the airfoil suction and pressure sides (indices: SS, PS) as well as the total TBL-TE noise should be evaluated separately according to:

$$L_{p(1/3)} = 10\log_{10}\left[10^{0.1L_{p(1/3),SS}} + 10^{0.1L_{p(1/3),PS}}\right]. \qquad (1)$$

Submitting authors are requested to adhere to the data file template *"CASE#{X}_{INSTITUTION}_FF_spectrum.dat"* in the "\templates" folder. For center frequencies where no reliable data can be provided write "9999" in the template. The choice of the frequency range is left to the authors. However, authors are highly encouraged to decrease the lower frequency limit of their simulation below the frequency limit of most of the available measurement data (f_c < 1 kHz). Frequency limits should be well-documented in the final reporting.

[2] Farfield 1/3-octave band TBL-TE noise directivity patterns $p_{rms}(\theta)$ *in Pa* and corresponding normalized directivities $p_{rms}/\overline{p_{rms}(\theta)}(\theta)$ with $\overline{p_{rms}(\theta)} := \frac{1}{2\pi}\int_0^{2\pi} p_{rms}(\theta)d\theta$ for r = 1 m, for center frequencies f_c = 1 kHz, f_c = 2 kHz, f_c = 5 kHz, f_c = 8 kHz, f_c = 10 kHz. If computationally affordable, consider steps of $\Delta\theta$ = 1°. A data template is provided with the file *"CASE#{X}_{INSTITUTION}_FF_directivity.dat".*

[3] Chordwise distributions of the time-averaged mean surface pressure coefficient $c_p(x_1/l_c)$ **(data available for cases #1 to #3)** and skin friction coefficient $c_f(x_1/l_c)$ on both sides of the airfoil, see sample data file *"CASE#{X}_{INSTITUTION}_cp-cf.dat"*.

[4] TE flow characteristics at both the pressure and suction sides; see sample data files *"CASE#{X}_{INSTITUTION}_INTEGRAL_TBL_parameters_1.0038.dat"* and *"CASE#{X}_{INSTITUTION}_TBL_profile_data_1.0038.dat"* for the output data structure.

a. Mean velocity profiles $U_1(x_2)/U_\infty$ between $-0.25 \le x_2/l_c \le 0.25$ at **100.38 % l_c (data available for cases #1 to #4 at SS only)** (chord-normal orientation of the profiles according to Figure 1)

b. Integral boundary layer parameters in mm derived from these profiles at **100.38 % l_c (data available for cases #1 to #4 at SS only)**, boundary layer thickness δ, displacement thickness δ_1, momentum loss thickness δ_2 and TBL edge velocities U_e in m/s. For derivation of these parameters from the mean velocity profiles apply the definitions and procedure as summarized in Sections 2.1 and 2.3.1.

c. Chord-normal distributions of the normal Reynolds stresses non-dimensionalized with the free-stream velocity squared $\langle u_1^2(x_2)\rangle / U_\infty^2$, $\langle u_2^2(x_2)\rangle / U_\infty^2$, $\langle u_3^2(x_2)\rangle / U_\infty^2$ and the resulting turbulent kinetic energy $k_T(x_2)/U_\infty^2$ at **100.38 % l_c (data available for cases #1 to #4 at SS only).**

d. Similarly, chord-normal distributions of the isotropic turbulence mean dissipation rate $\varepsilon(x_2)$ in m²/s³ and longitudinal integral length scale $\Lambda_f(x_2)$ in mm shall be provided at **100.38 % l_c (data available for cases #1 to #4 at SS only)**. If CFD simulation is performed by RANS/URANS together with a two-equation turbulence model then k_T and ε are direct results of the simulation. For the isotropic integral length scale derivation following equation can be applied:

$$\Lambda_f = 0.4\frac{(k_T)^{3/2}}{\varepsilon}. \qquad (2)$$

In case of Reynolds Stress Model (RSM) based (U)RANS simulations the Reynolds stresses $\langle u_i^2 \rangle$ are available together with dissipation ε. The turbulence kinetic energy can then be calculated as:

$$k_T = 0.5\left[\langle u_1^2\rangle + \langle u_2^2\rangle + \langle u_3^2\rangle\right], \qquad (3)$$

for isotropic turbulence $\langle u_1^2\rangle = \langle u_2^2\rangle = \langle u_3^2\rangle = 2/3k_T$.

e. Participants should document details of how flow transition is handled in the simulation.

[5] Unsteady surface pressure (point) power spectral density G_{pp} in dB/Hz re 20 µPa at the airfoil suction and pressure sides at 99 % l_c shall be provided. See sample data file "CASE#{X}_{INSTITUTION}_WPF_PSD_0.99.dat". The choice of the frequency range as well as the simulation narrow band frequency bandwidth Δf is left to the authors. However, note that narrow band spectra of finite band width Δf will have to be normalized to Δf = 1 Hz (cf. Section 3.1.2).

2.3.1 Approximation of the TE boundary-layer thickness δ and edge velocity U_e from simulated near-wake profiles.

The widely used definition of δ as the position were the local velocity equals 99 % of the free stream velocity U_∞ is not applicable to boundary layers with pressure gradient. Moreover, similar definitions based on the boundary layer edge velocity U_e as a fixed percentage of the potential flow velocity at the wall (the latter can be approximated from c_p at the TE) will not produce consistent results when combining this rather arbitrary definition with the corresponding definitions of the integral length scales δ_1 and δ_2 (Section 2.1). To provide both consistency and comparability of the results applicants are requested to adhere to the procedure shown in Figure 3.

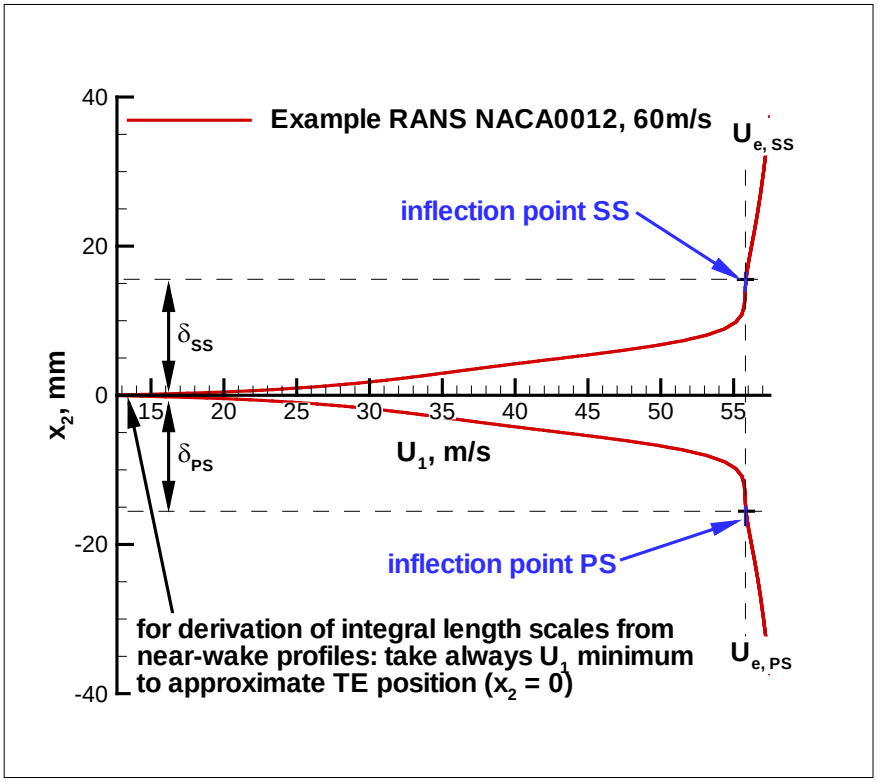

Figure 3: Determination of δ and U_e from the near wake mean flow profiles close to the TE.

Accordingly, δ at the TE is herein defined as the chord-normal distance from the U_1 minimum to the position of the inflection point between the TBL and the outer flow regime, and U_e is defined as the velocity at this position $U_1(\delta)$.

2.4. Reporting Format and Data File Structure

IMPORTANT: Participants are requested to send their contributions [1 and 2] to Michaela.herr@dlr.de until 31 May 2014 the latest. Authors who exceed this time limit will not be given the opportunity to present their results during the workshop (14-15th June, 2014).

[1] Tables of numerical results are requested timely prior to the workshop to facilitate an overall summary comparison between the results of all participants (done by the organizing team) and to allow for potential revisions or clarifications prior to the presentations. Contributors must adhere to the above parameter definitions, reporting instructions as well as to the data templates provided in the

"\templates" folder. For consistency an equivalent data file structure has been used for provision of the measured comparison data.

[2] Additionally, the participants are requested to furnish a **short documentation of 1-2 page(s)** which includes an overview on the used computational approach along with assumptions, limitations, and advantages as well as on major findings. The following topics should be addressed:

   a. Information on grid resolution, numerical error and CPU costs.

   b. Discussion of selected results that illustrate the relationship of flow characteristics to noise generation (i.e. effect of inflow velocity, angle of attack…). If computations are performed for the full matrix of test cases provide also a discussion comparing the results for the NACA0012 to those of the DU-96-180.

   c. In an outlook section, participants are requested to summarize their specific requirements of additional validation data that may be collected in a future measurement campaign dedicated to specific validation.

   A "SampleReportTemplate" is ready for download in the "\templates" folder.

[3] During the workshop participants are invited to present the above surveys on their used approach along with their major results and conclusions. Corresponding guidelines will be distributed in due time prior to the workshop.

3 Comparison Data

Selected experimental data sets are provided for test conditions close to the problem definition. To facilitate data usage, the TBL-TE noise and surface pressure spectra are scaled as far as possible according to the problem conditions for direct comparison and interpretation of the results. Scatter band estimates are provided through evaluation of experimental data from different test facilities and several organizations to roughly account for systematic errors resulting from uncertainties in setup specification, measurement techniques and data reduction.

3.1 Considered Data Sets

This section specifies the available data sets and the necessary scaling approaches that have been applied for direct comparison with the simulation results. Currently, data sets from (i) the Institute of Aerodynamics & Gas Dynamics (IAG) at the University of Stuttgart (ii) DLR Braunschweig and (iii) the University of Florida (UFL) have been made available for BANC-II/III. **Data owners of additional suitable data sets close to the problem statement are highly encouraged to contribute to the workshop; please contact michaela.herr@dlr.de to add your data sets to the statement.**
Moreover, the comprehensive NACA0012 data sets available at NASA Langley have led to the development of a NACA0012-based empirical airfoil noise prediction code by Brooks, Pope and Marcolini (BPM) [2]. Corresponding BPM predictions equivalent to the underlying scaled measurement data are also provided for comparisons (herein, predictions are derived by application of the free NREL software NAFNOISE [13] and are based on XFOIL calculations of the TBL parameters instead of the BPM-internal TBL-parameter prediction).

Summaries of the available comparison data can be found in the following reports as included in the “\documentation” or “\documentation\related papers” folders:

i) IAG data → \documentation\BANC-II-1_IAG_DATA_survey.pdf

ii) DLR data → Refs. [5], [6], [7]

iii) UFL data → \documentation\BANC-II-1_UFL_DATA_survey.pdf and Ref. [1]

iv) NASA data → Refs. [2], [13]

3.1.1 Farfield 1/3-Octave Band TBL-TE Noise Spectra, $L_{p(1/3)}(f_c)$

Noise data are provided for the original test parameters listed in

Table 2 but are also scaled according to the problem statement conditions for direct comparison with the simulation results. Herein, spectral scaling applies the following simplified relationships (indices 1,2 denote different test conditions):

$$L_{p(1/3)}(f_c)\Big|_{r_2,b_2,M_{\infty 2},\ldots TBL\ state_2} = L_{p(1/3)}(f_c)\Big|_{r_1,b_1,M_{\infty 1},\ldots TBL\ state_1} + 20\log_{10}\frac{r_1}{r_2} + 10\log_{10}\frac{b_2}{b_1}$$
$$+ 50\log_{10}\frac{M_{\infty 2}}{M_{\infty 1}} + 10\log_{10}\frac{\delta_{SS_2}+\delta_{PS_2}}{\delta_{SS1}+\delta_{PS1}} + 20\log_{10}\frac{T_{\infty 2}}{T_{\infty 1}} + 20\log_{10}\frac{\rho_{\infty 2}}{\rho_{\infty 1}} \qquad (4)$$

and

$$\frac{f_{c2}}{f_{c1}} = \frac{\delta_{SS_1}}{\delta_{SS2}}\ \frac{U_{\infty 2}}{U_{\infty 1}}\ . \qquad (5)$$

It is understood that this simplified scaling approach will not lead to a perfect collapse of measurement data collected within extended parameter ranges; however, for test conditions very close to the problem definition the resulting error is negligibly small (within the measurement repeatability) and affordable given the remaining systematic uncertainties in multiple trailing-edge noise data sets. Therefore, only those datasets will be used. The summarized data sets (original data with free-stream and TBL conditions according to

Table 2 and scaled data with free-stream and TBL condition adapted to the problem definition) are ready for download at \BANC-II-1\data\... in files \CASE#X\CASE#X_measurement-data_FF_spectrum.dat or \data\Tecplot files\ CASES#1-5_comparison-data_ALL_FF_spectrum.lpk. Both the original and scaled data sets are already normalized according to the reporting instructions summarized in Section 2.3 (b = 1 m, r = 1 m).

Table 2 provides measured or estimated (in brackets) positions for boundary layer transition. α corresponds to the aerodynamical angle of attack of the problem statement; wind tunnel geometrical angles-of-attack have been corrected to corresponding free air conditions.

The full data set is plotted in Figures 4 to 8. Selected data recommended for comparisons (the latter selection based on the good collapse of normalized spectra) are separately surveyed in Figure 9.

For similar test cases available data provided **a scatter band of roughly 3 dB which should be considered for all simulations.**

Table 2: Survey on provided test data for conditions close to the problem statement (data selected for "bracketing" experimental conditions).

# Airfoil	l_c, m	Boundary layer fixed transition position, fully turbulent downstream of x_1/l_c (SS: suction side, PS: pressure side)	U_∞, m/s M_∞, - Re, -	T_∞, K ρ_∞, kg/m³ p_∞, Pa Tu_{x1}, % u_∞	α, °	TE thickness, mm	Organization, (facility)
#1 NACA0012	0.4	SS: 0.065 PS: 0.065	50 0.1449 1.21 Mio	296.3 1.111 94496 0.05	0	0.22	IAG (LWT+SL) LWT: Laminar Wind Tunnel+ SL: Improved setup with acoustic lining
#1 NACA0012	0.4	SS: 0.065 PS: 0.065	60.0 0.1736 1.46 Mio	297.2 1.117 95295 0.05	0	0.22	IAG (LWT+SL)
#1 NACA0012	0.4	SS: 0.065 PS: 0.065	60.0 0.1772 1.57 Mio	285.4 1.156 94707 0.05	0	0.22	IAG (LWT)
#1 NACA0012	0.4	SS: 0.0925 PS: 0.0925	50.2 0.1458 1.29 Mio	294.9 1.188 100580 ~ 0.30	0	0.15	DLR (AWB)
#1 NACA0012	0.4	SS: 0.0925 PS: 0.0925	60.0 0.1742 1.54 Mio	295.7 1.185 100557 ~ 0.30	0	0.15	DLR (AWB)
#1 NACA0012	0.3	(SS: 0.05) (PS: 0.05)	52.4 0.1509 0.96 Mio	300 1.161 99000 .-	0	0.76	UFL (UFAFF)
#1 NACA0012	0.3	(SS: 0.05) (PS: 0.05)	59.4 0.1711 1.08 Mio	300 1.150 99000	0	0.76	UFL (UFAFF)

				.-			
#1 NACA0012	0.4	SS: 0.065 PS: 0.065	56.0 0.1664 1.50 Mio	281.5 1.181 95429 0.00	0		NASA BPM prediction [2] + XFOIL; NAFNOISE [13]
#2 NACA0012	0.4	SS: 0.065 PS: 0.065	60.0 0.1761 1.53 Mio	288.9 1.143 94790 0.05	4	0.22	IAG (LWT)
#2 NACA0012	0.3	(SS: 0.05) (PS: 0.05)	52.6 0.1512 0.96 Mio	301 1.146 99000 .-	2.1	0.76	UFL (UFAFF)
#2 NACA0012	0.3	(SS: 0.05) (PS: 0.05)	59.6 0.1714 1.08 Mio	301 1.146 99000 .-	2.1	0.76	UFL (UFAFF)
#2 NACA0012	0.4	SS: 0.065 PS: 0.065	54.8 0.1641 1.50 Mio	278.0 1.190 94975 0.00	4		NASA BPM prediction [2] + XFOIL; NAFNOISE [13]
#2,#3 NACA0012	0.4	(SS: 0.0756) (PS: 0.0925)	50.2 0.1456 1.29 Mio	295.3 1.185 100478 ~ 0.30	5	0.15	DLR (AWB)
#2,#3 NACA0012	0.4	(SS: 0.0696) (PS: 0.0925)	60.0 0.1741 1.54 Mio	295.6 1.184 100459 ~ 0.30	5	0.15	DLR (AWB)
#3 NACA0012	0.4	SS: 0.060 PS: 0.070	60.0 0.1761 1.53 Mio	288.9 1.143 94790 0.05	6	0.22	IAG (LWT)
#3 NACA0012	0.4	(SS: 0.0298) (PS: 0.0925)	50.0 0.1454 1.29 Mio	294.6 1.188 100486	7.6	0.15	DLR (AWB)

				~ 0.30			
#3 NACA0012	0.4	(SS: 0.0276) (PS: 0.0925)	59.9 0.1739 1.54 Mio	294.9 1.196 101265 ~ 0.30	7.6	0.15	DLR (AWB)
#3 NACA0012	0.4	SS: 0.060 PS: 0.070	53.0 0.1597 1.50 Mio	273.8 1.224 96188 0.00	6		NASA BPM prediction [2] + XFOIL; NAFNOISE [13]
#4 NACA0012	0.4	SS: 0.065 PS: 0.065	40.0 0.1157 1.00 Mio	297.4 1.107 94506 0.05	0	0.22	IAG (LWT+SL)
#4 NACA0012	0.4	SS: 0.0925 PS: 0.0925	40.1 0.1169 1.05 Mio	292.1 1.199 100566 ~ 0.30	0	0.15	DLR (AWB)
#4 NACA0012	0.3	(SS: 0.05) (PS: 0.05)	34.9 0.1007 0.65 Mio	346.64 1.165 100000 .-	0.1	0.76	UFL (UFAFF)
#4 NACA0012	0.3	(SS: 0.05) (PS: 0.05)	42.0 0.1210 0.78 Mio	347.22 1.161 100000 .-	0.1	0.76	UFL (UFAFF)
#4 NACA0012	0.4	SS: 0.065 PS: 0.065	37.7 0.1118 1.00 Mio	283.1 1.171 95156 0.00	0		NASA BPM prediction [2] + XFOIL; NAFNOISE [13]
#5 DU-96-180	0.3	SS: 0.12 PS: 0.15	60.0 0.1730 1.13 Mio	299.3 1.164 100004 ~ 0.30	4	0.3	DLR (AWB)

According to a literature review on available data sets some of the relevant TBL-TE noise data had been acquired at smaller chord (~0.2 m) NACA0012-like airfoil sections (conditions for the former BANC-I problem statement). However, the

corresponding data sets were lacking supplementing aerodynamical data and test conditions (like transition locations, detailed TE geometry…), were in parts incompletely documented and/or corresponding raw data files from earlier test campaigns had not been stored. Some of the wind-tunnel models provided blunt TE geometries and hence, supported also the occurrence of vortex shedding from the TE, a noise generation mechanism which is not covered by the current problem statement with focus on broadband TBL-TE noise. To provide at least a rough estimate of expected systematic errors among different experimental groups, test facilities, measurement techniques and/or post processing methods also NACA0012 test data for a ~0.2 m chord length have been considered (not shown here) and confirmed the herein shown ~3-dB systematic scatter for similar configurations. Direct scaling of these data according to the problem statement is not recommended because the per se imperfect scaling procedure itself would induce an additional systematic error on the scaled noise spectra.

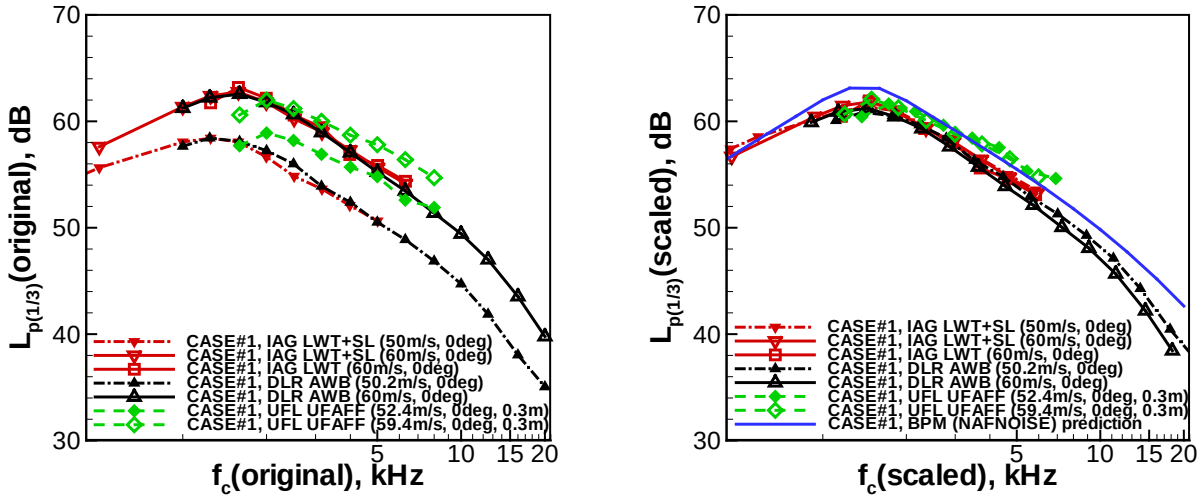

Figure 4: Available comparison data close to case #1 in reporting format; left: original data at different test conditions (scaled to r = b = 1 m only), right: data scaled to problem statement conditions and corresponding NAFNOISE (BPM) predictions.

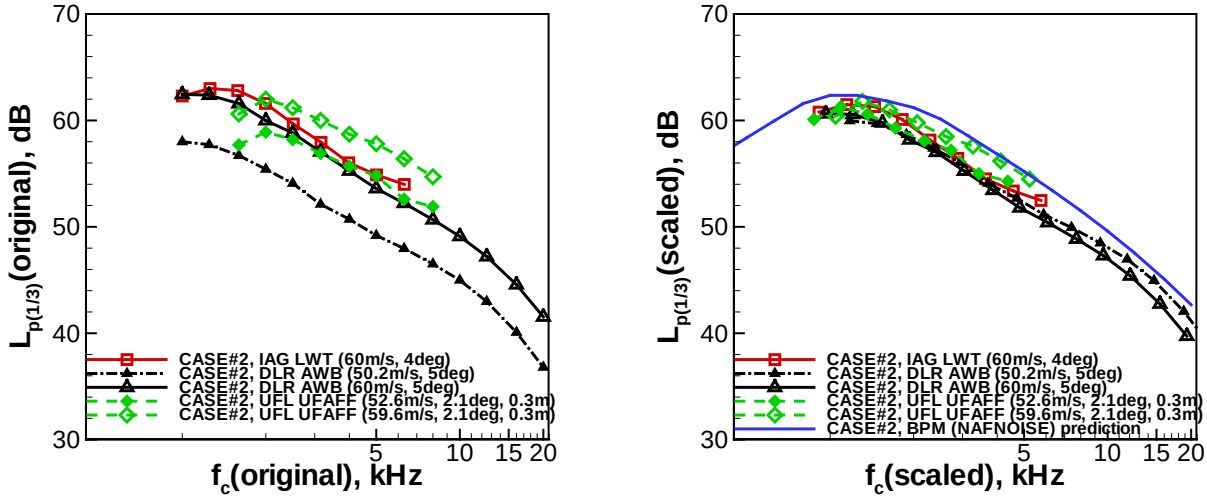

Figure 5: Available comparison data close to case #2 in reporting format; left: original data at different test conditions (scaled to r = b = 1 m only), right: data scaled to problem statement conditions and corresponding NAFNOISE (BPM) predictions.

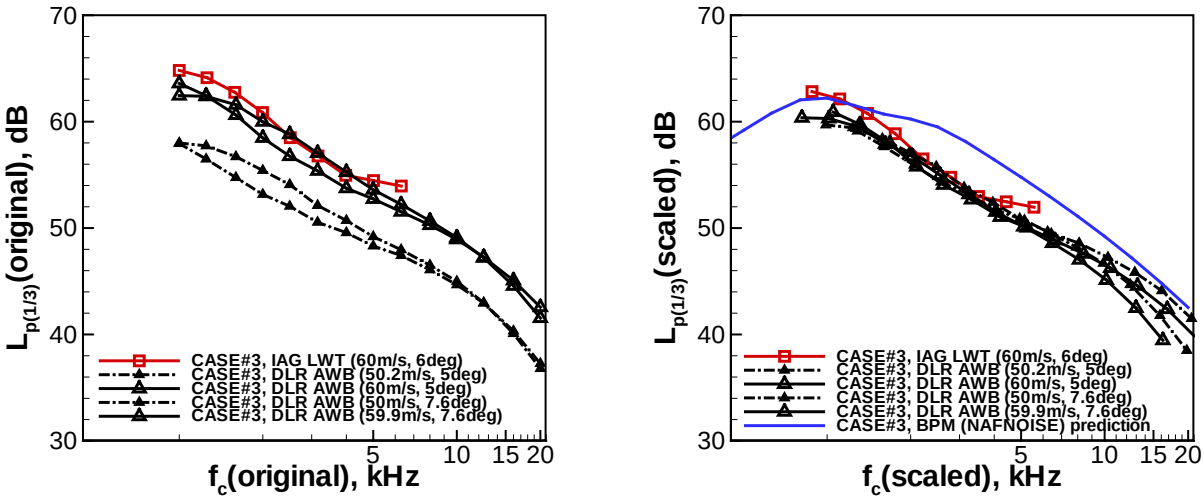

Figure 6: Available comparison data close to case #3 in reporting format; left: original data at different test conditions (scaled to r = b = 1 m only), right: data scaled to problem statement conditions and corresponding NAFNOISE (BPM) predictions.

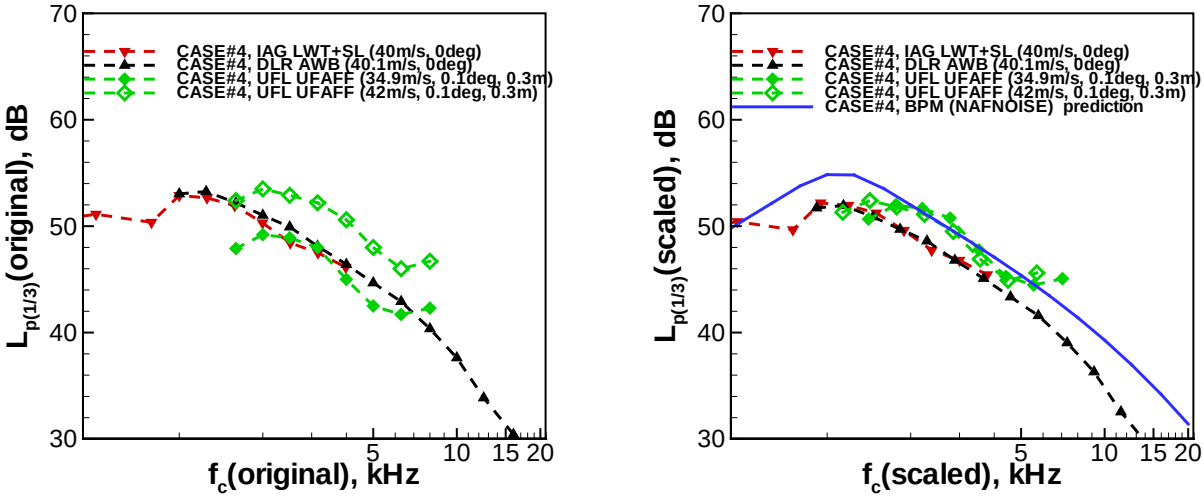

Figure 7: Available comparison data close to case #4 in reporting format; left: original data at different test conditions (scaled to r = b = 1 m only), right: data scaled to problem statement conditions and corresponding NAFNOISE (BPM) predictions.

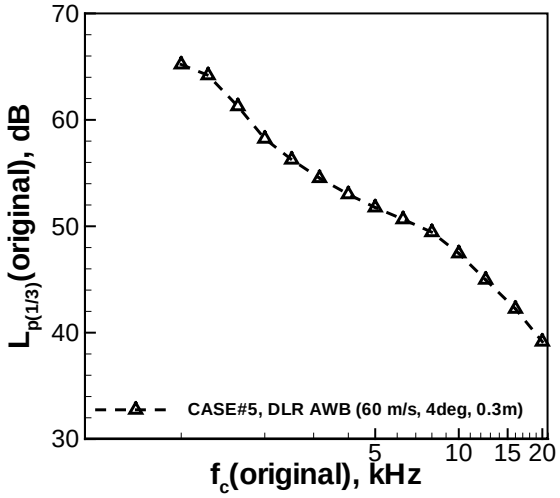

Figure 8: Available comparison data for case #5 in reporting format (scaled to r = b = 1 m, original data correspond to problem statement conditions).

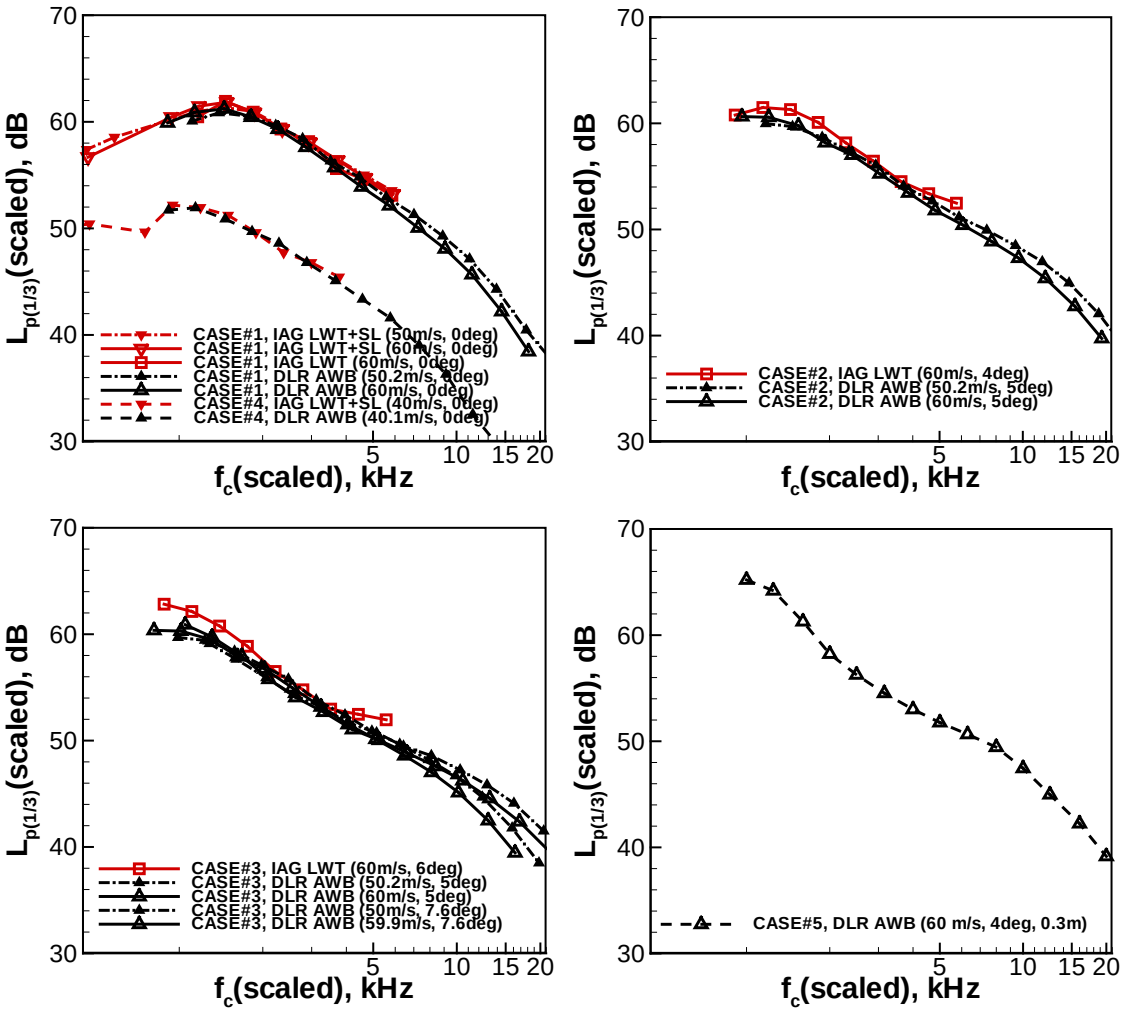

Figure 9: Survey of the recommended comparison datasets for cases#1-5.

3.1.2 Wall Pressure Point Frequency Spectra, $G_{pp}(f)$

For the NACA0012 airfoil, besides farfield TBL-TE noise spectra, the unsteady wall pressure point frequency spectra at 98.9% chord are also available from Refs. [9][10]. These datasets are summarized in Table 3. As done for the TBL-TE farfield spectra both unscaled (conditions as in Table 3, but data format according to section 2.3) and scaled data are provided in files \CASE#X\CASE#1_measurement-data_WPF_PSD.data or \Tecplot files\CASES#1-4_comparison-data_WPF_PSD_IAG_SS_PS.lpk at \BANC-II-1\data\.... Note that these data are provided with and without sensor resolution correction according to Corcos [4], the latter (variable "G_pp,Corcos(scaled), dB/1Hz") recommended for comparisons (cf. Figure 10).

For comparisons with the numerical results measured narrow band spectra of finite band width Δf = 10.8 Hz have been normalized to Δf = 1Hz and approximately scaled to the problem statement conditions applying Eqs. (6-7):

$$G_{pp}(f)\Big|_{M_{\infty 2},\ldots TBL\ state_2,\Delta f_2=1\,\mathrm{Hz}} = G_{pp}(f)\Big|_{M_{\infty 1},\ldots TBL\ state_1,\Delta f_1} + 10\log_{10}\frac{1\mathrm{Hz}}{\Delta f_1} + 30\log_{10}\frac{M_{\infty 2}}{M_{\infty 1}} + 10\log_{10}\frac{\delta_{SS2}}{\delta_{SS1}} + 20\log_{10}\frac{T_{\infty 2}}{T_{\infty 1}} + 20\log_{10}\frac{\rho_{\infty 2}}{\rho_{\infty 1}} \quad (6)$$

and

$$\frac{f_2}{f_1} = \frac{\delta_{SS_1}}{\delta_{SS2}} \frac{U_{\infty 2}}{U_{\infty 1}} \quad . \tag{7}$$

Eqs. (6) and (7) are valid for the WPF spectrum at the suction side (index SS); equivalent expressions hold for the pressure side if SS properties are replaced by PS properties (exchange index SS by PS in the Eqs.).

Table 3: Survey on provided WPF test data for conditions close to the problem statement (data selected for "bracketing" experimental conditions).

# Airfoil	l_c, m	Boundary layer fixed transition position, fully turbulent downstream of x_1/l_c (SS: suction side, PS: pressure side)	U_∞, m/s M_∞, - Re, -	T_∞, K ρ_∞, kg/m³ p_∞, Pa Tu_{x1}, % u_∞	α, °	TE thickness, mm	Organization, (facility)
#1 NACA0012, PS & SS	0.4	SS: 0.065 PS: 0.065	62.1 0.1803 1.50 Mio	295.3 1.102 93365 0.05	0	0.22	IAG (LWT)
#2 NACA0012, PS & SS	0.4	SS: 0.065 PS: 0.065	62.1 0.1803 1.50 Mio	295.3 1.102 93365 0.05	4	0.22	IAG (LWT)
#3 NACA0012, PS & SS	0.4	SS: 0.060 PS: 0.070	62.1 0.1803 1.50 Mio	295.3 1.102 93365 0.05	6	0.22	IAG (LWT)
#4 NACA0012, SS only	0.4	SS: 0.065 PS: 0.065	41.0 0.1188 1.00 Mio	296.5 1.116 94986 0.05	0	0.22	IAG (LWT)

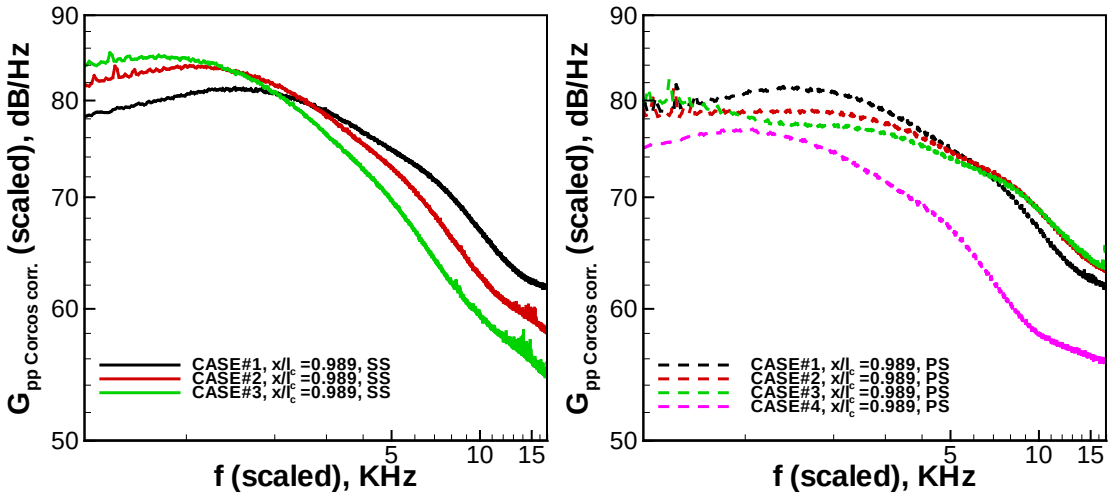

Figure 10: Survey of recommended comparison WPF spectra for cases#1-4; left: suction side (SS), right: pressure side (PS), corresponding data file at \data\Tecplot files\ CASES#1-4_comparison-data_WPF_PSD_IAG_SS_PS.lpk.

3.1.3 Aerodynamics and Turbulent Boundary-Layer Parameters

Test data sets corresponding to the problem statement definition are listed in Table 4.

Table 4: Survey on test conditions for available TBL parameters and cp distribution data.

# Airfoil	l_c, m	Boundary layer fixed transition position, fully turbulent downstream of x_1/l_c (SS: suction side, PS: pressure side)	U_∞, m/s M_∞, - Re, -	T_∞, K ρ_∞, kg/m³ p_∞, Pa Tu_{x1}, % u_∞	α, °	TE thickness, mm	Organization, (facility)
#1 NACA0012, TBL@SS only	0.4	SS: 0.065 PS: 0.065	56.0 0.1664 1.50 Mio	281.5 1.181 95429 0.05	0	0.22	IAG (LWT)
#2 NACA0012, TBL@SS only	0.4	SS: 0.065 PS: 0.065	54.8 0.1641 1.50 Mio	278.0 1.190 94975 0.05	4	0.22	IAG (LWT)
#3 NACA0012, TBL@SS only	0.4	SS: 0.060 PS: 0.070	53.0 0.1597 1.50 Mio	273.8 1.224 96188 0.05	6	0.22	IAG (LWT)

#4 NACA0012, TBL@SS only, no c_p data	**0.4**	**SS: 0.065 PS: 0.065**	**37.7 0.1118 1.00 Mio**	**283.1 1.171 95156 0.05**	**0**	**0.22**	**IAG (LWT)**

These data are ready for download at \BANC-II-1\data\... in files \CASE#X \CASE#X_TBL_profile_data_1.0038.dat and \CASE#X\CASE#1_cp.dat or in \data \Tecplot files\CASES#1-4_TBL_profile_data_IAG_SS.lpk and \CASES#1-5_cp-distributions_IAG-XFOIL.lpk.

The files \CASE#X\CASE#X_TBL_profile_data_1.0038.dat contain measured values for $U_1(x_2)$ and $U_1(x_2)/U_\infty$, measured anisotropic Reynolds stresses $\langle u_i^2(x_2)\rangle$ and $\langle u_i^2(x_2)\rangle / U_\infty^2$ and turbulence kinetic energy $k_T(x_2)$ and $k_T(x_2)/U^2_\infty$ but also equivalent modeled isotropic Reynolds stresses derived from the anisotropic measurement data (Variable: $2/3k_T$ (model)), modeled $\varepsilon(x_2)$ and $\Lambda_f(x_2)$. Additionally to the requested simulation parameters integral length scales $\Lambda_{11,2}(x_2)$ and $\Lambda_{22,2}(x_2)$ applying two different model approaches are included for interested participants (see Section 3.3). The detailed modeling procedures are documented in Refs. [11], [12].

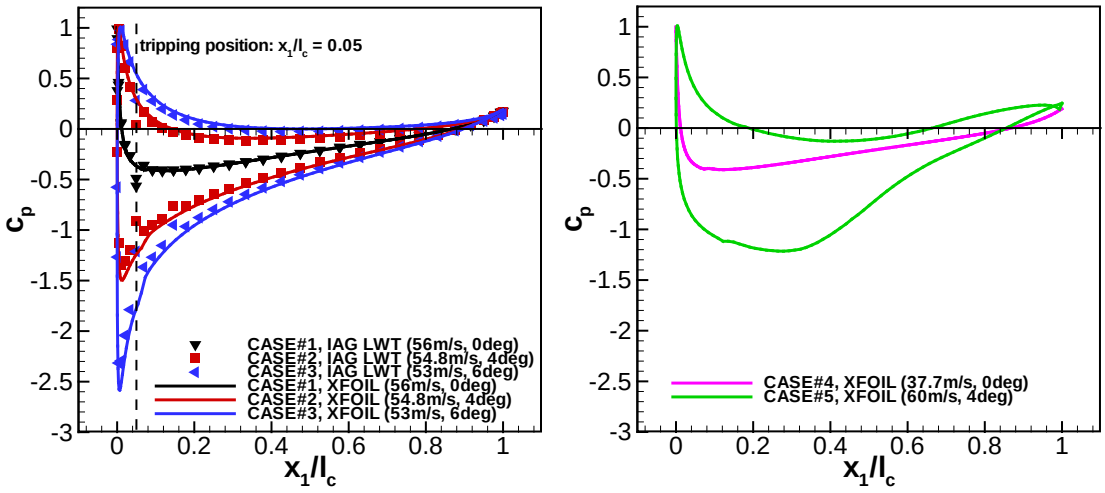

Figure 11 (left): Survey on available cp distribution data for CASES#1-3 compared to XFOIL calculation data, right: XFOIL calculation data for remaining CASES#4-5 (no measurement data available).

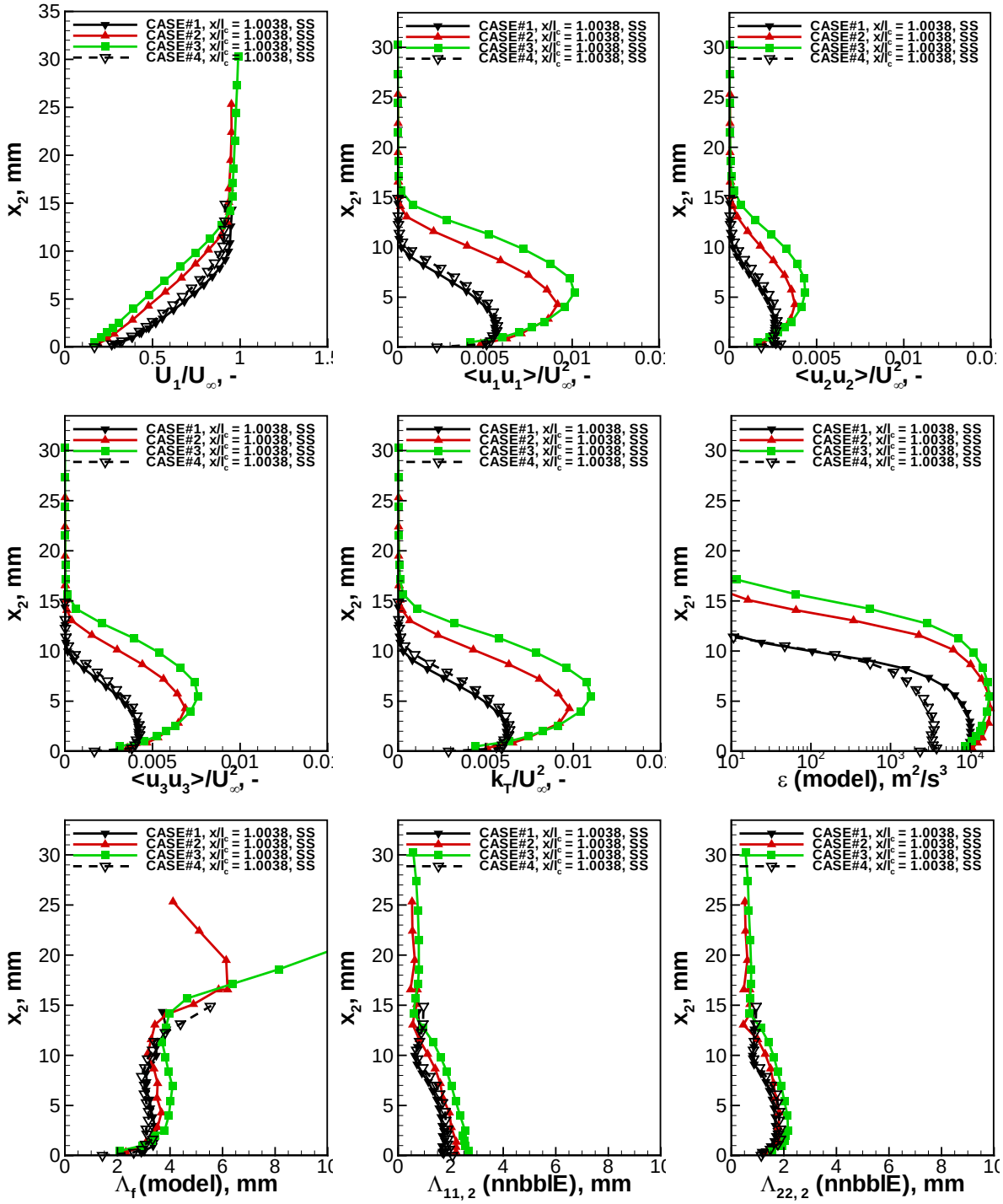

Figure 12: Survey on available TBL data (SS) for CASES#1-4 (corresponding data file at \data\Tecplot files\CASES#1-4_TBL_profile_data_IAG_SS.lpk).

3.3 Additional Data

- Limited additional two-point correlation data at various chord-normal positions x_2 and fixed chord position x_1/l_c = 1.0038 for test cases #1 to #4 (Table 4) are available. These data include $R_{11}(x_1, x_2 + \xi_2, x_3)$, $R_{22}(x_1, x_2 + \xi_2, x_3)$ maps and related integral length scales $\Lambda_{ii,n}(x_2)$ of the u_1 and u_2 velocity components for separation in x_2-direction (selected data have been already included in the files \data\CASE#X \CASE#X_TBL_profile_data_1.0038.dat.
- Additionally, corresponding single-point one-dimensional velocity spectra $\varphi_{11}(k_1)$ and $\varphi_{22}(k_1)$ at various x_2-positions are also available.
- Measurement data of the wall pressure fluctuation point frequency spectrum (cf. Table 3) also provide frequency-dependent span-wise coherence length scales of the fluctuating pressure $\Lambda_{p,3}(f)$.

Interested participants are requested to directly contact Mohammad Kamruzzaman, mktupa@gmail.com (in Cc.: michaela.herr@dlr.de), for more information.

4 References

[1] Bahr, C., Li, J. and Cattafesta, L., “Aeroacoustic Measurements in Open-Jet Wind Tunnels – An Evaluation of Methods Applied to Trailing Edge Noise”, AIAA Paper 2011-2771, 2011 → \documentation

[2] Brooks, T. F., Pope, D. and Marcolini, M. A., “Airfoil Self-Noise and Prediction”, Reference Publication 1218, NASA, 1989 → \documentation

[3] Brooks, T. F. and Hodgson, T. H., “Trailing Edge Noise Prediction from Measured Surface Pressures,” Journal of Sound and Vibration, Vol. 78, No. 1, 1981, pp. 69–117 → \documentation

[4] Corcos, G. M., “Resolution of Pressure in Turbulence,” Journal of the Acoustical Society of America, Vol. 35, No. 2, 1963, pp. 192–199. → \documentation

[5] Herr, M., “Design Criteria for Low-Noise Trailing -Edges,” AIAA Paper 2007-3470, 2007 → \documentation

[6] Herr, M., “Trailing-Edge Noise Data Quality Assessment for CAA Validation,” AIAA Paper 2010-3877, 2010 → \documentation

[7] Herr, M., “In Search of Airworthy Trailing-Edge Noise Reduction Means,” AIAA Paper 2011-2780, 2011 → \documentation

[8] Herrig, A., Wuerz, W., Kraemer, E., and Wagner, S., “New CPV-Results of NACA0012 Trailing-Edge Noise”, Novosibirsk, 30.06.-06.07. 2008. Int. Conference on Methods of Aerophysical Research (ICMAR) → \documentation

[9] Herrig, A., Kamruzzaman, M., Wuerz, W., and Wagner, S., “Broadband Airfoil Trailing-Edge Noise Prediction from Measured Surface Pressures and Spanwise Length Scales”, International Journal of Aeroacoustics, Vol. 12, No. 1–2, 2013, pp. 53–82

[10] Herrig, A., “Validation and Application of a Hot-Wire based Method for Trailing-Edge Noise Measurements on Airfoils”, Doctoral thesis, Faculty of Aerospace Engineering and Geodesy, University of Stuttgart, 2011

[11] Kamruzzaman, M., Lutz, T., Würz, W., Kraemer, E., “On the Length Scales of Turbulence for Aeroacoustic Applications,” AIAA Paper 2011-2734, 2011 → \documentation

[12] Kamruzzaman, M., Lutz, T., Herrig, A., Kraemer, E., “Semi-Empirical Modeling of Turbulent Anisotropy for Airfoil Self Noise Prediction”, AIAA Journal, Vol. 50, No 1, 2012, pp. 46–60 → \documentation

[13] Moriarty, P., “NAFNoise User’s Guide,” Technical Report, National Wind Technology Center, National Renewable Energy Laboratory, Golden, CO, July 2005. → \documentation

[14] Rossignol, K.-S. et al.: previously unpublished data acquired by DLR Braunschweig (GE proprietary, released for BANC-II by courtesy of GE Energy), 2011

The accordingly marked reports can be found in the “\documentation\related papers” folder.